Colloid Polym Sci 277:557–562 (1999)

ORIGINAL CONTRIBUTION

S.L. Koontz
R.V. Devivar
W.J. Peltier
J.E. Pearson
T.A. Guillory
J.D. Fabricant

The pellicular monolith: pore-surface functionalization and surface-phase construction in macroporous polymeric materials

Received: 20 November 1998
Accepted in revised form: 21 January 1999

S.L. Koontz (✉) · R.V. Devivar
W.J. Peltier · J.E. Pearson · T.A. Guillory ·
J.D. Fabricant
FlowGenix Corporation, 100 E. NASA
Road 1, Suite 102, Webster, TX 77598,
USA

Abstract We report synthesis and characterization of a macroporous polymeric material containing a covalently immobilized pore-surface phase of well-defined thickness, gel-phase porosity and organic functional group content. The pore surfaces of otherwise inert macroporous (32 μm mean pore size) ultrahigh-molecular-weight polyethylene (UHMWPE) are aminated throughout using a low-pressure flowing-discharge process to enable covalent immobilization of lightly cross-linked polymer colloid particles on all pore surfaces in the monolith. Solvent swelling and chemical derivitization of the covalently immobilized polymer colloid particles produce a pore-surface gel phase of well-defined thickness, organic amine content, and gel-phase porosity. The low degree of cross-linking in the polymer colloid particles prevents dissolution of the immobilized colloid in good solvents and enables the formation of pore-surface gel phases having high gel porosity on swelling in good solvents. The pore-surface amination introduced by the flowing discharge process varies by less than 17% through 5-mm thickness of the macroporous UHMWPE material. The properties of the pore-surface gel phase also vary by less than 17% through the cross section. The pore-surface immobilized polymer colloid particles swell by a factor of 10 in water and tetrahydrofuran after derivitization with polyethylene glycol.

Key words Latex – Polymer colloid – Macroporous – Polymer surface chemistry modification – Polymer gels

Introduction

Pellicular chromatographic column packing beads are characterized by a surface phase mounted on an essentially nonporous bead [1]. Similarly, a pellicular monolith is a macroporous solid, made of essentially nonporous structural elements, which acts as a structural support for a covalently immobilized pore-surface phase. The first step in construction of the pellicular monolith is making the otherwise inert pore surfaces of the macroporous polyethylene (PE) reactive using ammonia flowing-discharge radical chemistry (FDRC) [2–4] to place covalently immobilized amine functionalities on all the pore surfaces. Next, the FDRC aminated pores are filled with a surfactant-stabilizer aqueous dispersion of 0.46 μm diameter polymer colloid particles [5] that react to become covalently coupled to the aminated pore surfaces. Finally, the pore-surface gel phase is produced by solvent swelling and derivitizing the immobilized polymer colloid particles.

Covalently cross-linked porous polymers constitute a large family of materials with applications in the areas of separations, solid-phase synthesis, and catalysis [6]. Cross-linked porous polymeric materials can be placed in one of two categories on the basis of the macromolecular architecture of the material: (1) "microporous gels" which exhibit porosity only on swelling with solvent, and (2) macroporous polymers characterized by a permanent porous structure which persists in the dry state [6]. The pellicular monolith reported here combines features of both structural categories in that a gel phase is mounted on the pore surfaces of a macroporous solid.

Various solution and gas-phase processes have been reported to produce useful chemical modifications of polymers [7–16]. Most previously reported methods produce significant collateral damage to the polymer, while producing only limited concentrations of the desired functional groups [7–16]. Of the previously reported methods for modifying polymer surface chemistry, low-pressure plasma discharge chemistry is most similar to the FDRC reported here. The downstream or flowing-discharge process differ from in-plasma methods by enabling the reaction of the plasma-generated gaseous radicals with polymer surfaces at positions remote from the plasma environment used to produce the gaseous radicals [8, 9, 12, 15, 16].

The most important gas-phase reactants in the ammonia FDRC process are atomic hydrogen, amino radical and imino radical. The chemistry of the ammonia FDRC process is summarized in the following reaction scheme.

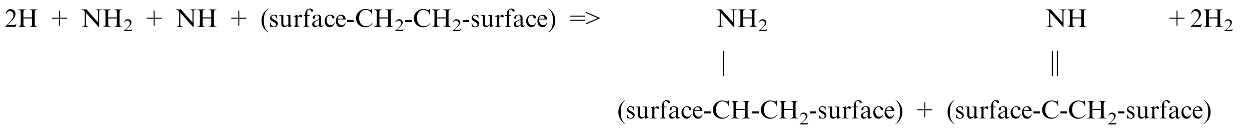

$$2H + NH_2 + NH + (\text{surface-}CH_2\text{-}CH_2\text{-surface}) \Rightarrow \underset{(\text{surface-CH-}CH_2\text{-surface})}{\overset{NH_2}{|}} + \underset{(\text{surface-C-}CH_2\text{-surface})}{\overset{NH}{\|}} + 2H_2$$

Analysis of critically reviewed data on the kinetics of atomic hydrogen, amino radical and imino radical reactions with aliphatic hydrocarbon vapors [17] suggests that hydrogen atom abstraction by atomic hydrogen is the primary reaction event and that imino and amino radicals react with the resulting hydrocarbon radical sites.

Reaction of ammonia FDRC-treated porous PE with a polymer colloid, followed by chemical derivitization, produces the pore-surface gel phase in the pellicular monolith. The polymer colloid particles used in this are random copolymers of styrene and (chloromethyl)styrene. A limited number of the benzyl chloride residues on the exterior of the colloid particles react directly with the nucleophilic amine functions on the ammonia FDRC-treated macroporous ultrahigh-molecular-weight PE (UHMWPE) material to covalently couple the colloid particles to the aminated pore surfaces (see reaction scheme below).

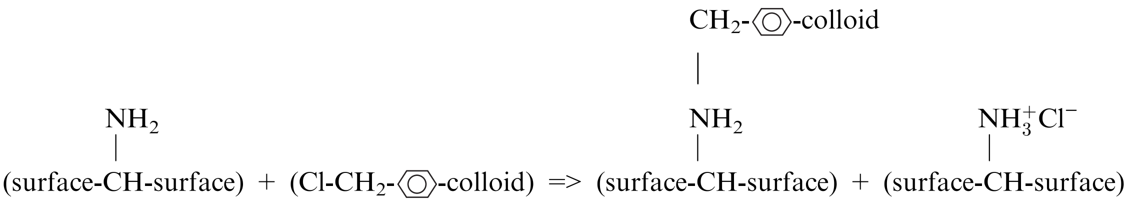

The diameter of the polymer colloid particles and the degree of cross-linking determine the ultimate thickness (i.e., change in pore size of the macroporous matrix) and the gel porosity (i.e., molecular size-exclusion properties) of the immobilized pore-surface gel phase. Some cross-linking is needed in the polymer particles to prevent simple dissolution of the immobilized polymer colloid, except for the few chains covalently coupled directly to the pore surface, in a good solvent. The thickness of the pore-surface gel phase after solvent swelling determines the change in the nominal pore size of the porous solid and therefore the change in resistance to fluid flow.

Materials, methods and apparatus

The pore surfaces of macroporous UHMWPE materials were aminated using FDRC apparatus and methods similar to those already described [2–4] with the exception that ammonia was used instead of oxygen as the process gas.

The macroporous UHMWPE materials used in this work, Porex X-4920 and Porex T^3, are manufactured by Porex Technologies (Fairburn, Georgia, USA). The Porex X-4920 material has a nominal pore size of 30 μm and a thickness of 15,875 μm (0.15875 cm) while T^3 material has a nominal pore size of 7 μm and a thickness of 6,550 μm (0.0655 cm).

Polymer colloid was purchased as a custom synthesis product from Bang's Laboratories, Fishers, Indiana, USA. The polymer composition was specified as 50% styrene, 49.8% (chloromethyl) styrene, and 0.2% divinylbenzene with a particle size of 0.46 μm as a surfactant-stabilized colloidal dispersion in water (10% solids by weight). Polymer colloid was diluted tenfold in pH 8.0 50 mM sodium phosphate buffer for covalently coupling to the pore surfaces of the aminated macroporous UHMWPE. The coupling reaction ran for 1 h at 55 °C. Covalent coupling was verified by measurement of the specific weight gain of the UHMWPE material after washing and extensive extraction with tetrahydrofuran (THF).

Fluorescein isothiocyanate (FITC isomer I) and 5-(4,6-dichlorotriazinyl)aminofluorescein (5-DTAF) were obtained from Molecular Probes, Eugene, Oregon, USA. Solutions of FITC and 5-DTAF used for detecting reactive alkyl amine or alkyl hydroxyl groups on FDRC-treated porous UHMWPE material were prepared as follows. Typically, 10 mg FITC or 5-DTAF was first dissolved in 1 cm^3 99.8% pure anhydrous *N*, *N*-dimethylformamide (DMF, Aldrich). The resulting DMF solution was then diluted to 10 cm^3 with pH 8.0, 50 mM sodium phosphate buffer. Propylamine (99% + pure, Aldrich) and 2-aminopentane (99% + pure, Aldrich) were used to block the amine reactive functional groups in FITC and 5-DTAF in control studies by simply adding a molar excess of the amines (10 mg/ml) to the FITC or 5-DTAF reactive staining solutions and allowing the mixture to stand overnight at room temperature prior to use.

FITC-stained ammonia FDRC Porex samples (and controls) were also subjected to base hydrolysis in 0.1 M NaOH in deionized water at 55 °C in the dark until the optical density of the supernatant reached a plateau. Subsequently, the optical density of the supernatant solution was determined with a Hewlett-Packard model 8453 spectrophotometer. The optical absorbance at 490 nm was then used to calculate the number of moles of fluorescein amine released from the Porex materials by the base hydrolysis. The extinction coefficient of the FITC hydrolysis product was 7.5×10^4 l $(\mathrm{mol\ cm})^{-1}$.

Surface amine groups on ammonia FDRC Porex were converted to amides using Cap A and Cap B solutions which were obtained from Perspective Biosystems (Hamburg, Germany). Cap A is a solution of pyridine and 1-methylimidizole in THF. Cap B is a solution of acetic anhydride in THF. The capping reaction is simple *N*-acetylation.

Triethylene glycol diamine (Jeffamine XTJ-504) was obtained from Huntsman Chemicals (Austin, Texas, USA) and was used as received. Triethylene glycol diamine (5 g) was dissolved in 17.5 cm^3 dry, stabilized THF (OmniSolv, stabilized with 250 ppm BHT, EM Science, Gibbstown, New Jersey, USA) containing 2.5 cm^3 anhydrous DMF for primary derivitization of the (chloromethyl)styrene functions in the immobilized polymer colloid particles prior to reaction with fluorescein-polyethylene glycol (PEG) *N*-hydroxy succinimide (NHS) ester.

The low polydispersity ($M_w/M_n = 1.06$) NHS ester of fluorescein PEG carboxylic acid (MW 5000) were obtained from Shearwater Polymers (Huntsville, Alabama, USA). The Shearwater fluorescein-PEG-NHS ester was used as received. The fluorescein-PEG-NHS ester was dissolved in 10% anhydrous DMF in THF for reaction with the pore-surface gel phase, which was conducted overnight at room temperature with stirring and then extracted extensively with THF and water.

Primary characterization of FDRC surface chemistry was accomplished by X-ray photoelectron spectroscopy (XPS) at Charles Evans Associates (Redwood City, California, USA). Diffuse reflectance fourier transform infrared spectroscopy (DRIFT) was also used as a surface chemistry characterization method. XPS is a more surface sensitive technique than DRIFT. The DRIFT sampling depth is on the order of 1 μm while the sampling depth of XPS is of the order of 100 Å [18].

The pore size distribution and surface area of Porex X-4920 and Porex T^3 were determined by both mercury intrusion porosimetry and krypton gas adsorption at Micromeritics, Norcross, Georgia, USA.

Results and discussion of results

In the present study we fully functionalized the interstitial pore surfaces of two different types of macroporous UHMWPE filter materials: Porex X-4920 and Porex T^3. The average pore diameters determined by mercury intrusion porosimetry were 28.3 μm for Porex X-4920 and 7.7 μm for Porex T^3. The total pore-surface areas by mercury porosimetry were 1080 cm^2/g for X-4920 and 3980 cm^2/g for T^3. The surface areas measured by krypton gas adsorption were 1407 cm^2/g for X-4920 and 2460 cm^2/g for T^3. A scanning electron photomicrograph of the 32-μm pore-size material is shown in Fig. 1. The interparticle porosity, ε, of Porex X-4920 was determined to be 0.425 by density measurement.

Comparison of XPS and DRIFT spectra shows that the FDRC surface modification was limited to the molecular surface of the material. The XPS spectra of ammonia FDRC Porex T^3 demonstrated an increase in the surface nitrogen content to 8.1 atom% from 0.0 atom% in the untreated control. There was no corresponding change (at the level of 0.01 absorbance units) in the DRIFT spectrum in general or in the amine region (3200–3400 cm^{-1}) in particular, indicating that the bulk polymer beneath the surface layer was unaffected by the FDRC treatment [18].

The ammonia FDRC-modified macroporous UHMWPE material became reactive with the amine reagents FITC and 5-DTAF. These reactions were blocked, either by prior treatment of the ammonia FDRC-treated material with acetic anhydride/l-methylimidazole in THF (to convert surface amine groups to amides), or by prior treatment of the FITC or DTAF with either 2-amino pentane or propylamine which block the isothiocyanate or triazinyl chloride functionalities.

These staining experiments ruled out nonspecific adsorption of the reactive dyes and demonstrate the presence of covalently immobilized functional groups on the FDRC-activated pore-surfaces which show the chemical reactivity expected for organic amine groups. The FDRC-treated materials were modified throughout the outer and interstitial pore surfaces, in as much that they stained completely with FITC and DTAF as determined by visual examination of cross sections of the materials. Photographs of the stained FDRC materials and the corresponding controls are shown in Fig. 2.

A quantitative assessment of the uniformity of the ammonia FDRC surface modification through the cross section of the porous UHMWPE material was performed by stacking disks of the Porex X-4920 in short glass tubes. In this configuration, the reactive FDRC gases had to diffuse into the disk stack from the side facing the FDRC gas stream, i.e., through the top disk and the middle disk to the bottom disk. The degree of FDRC amination of the top, middle, and bottom disk were compared by measuring: (1) FITC reaction assay, (2) covalent polymer colloid coupling, and (3) colloid coupling with subsequent derivitization by the 5000 MW fluorescein-PEG-NHS as shown in the following reactions schemes [19].

The results of the FITC and colloid coupling experiments on the top disk, exposed directly to the FDRC environment, the middle disk, and the bottom disk are summarized in Table 1. The results show that the degree of surface amination is essentially the same throughout the disk stack. The uniform weight gain on

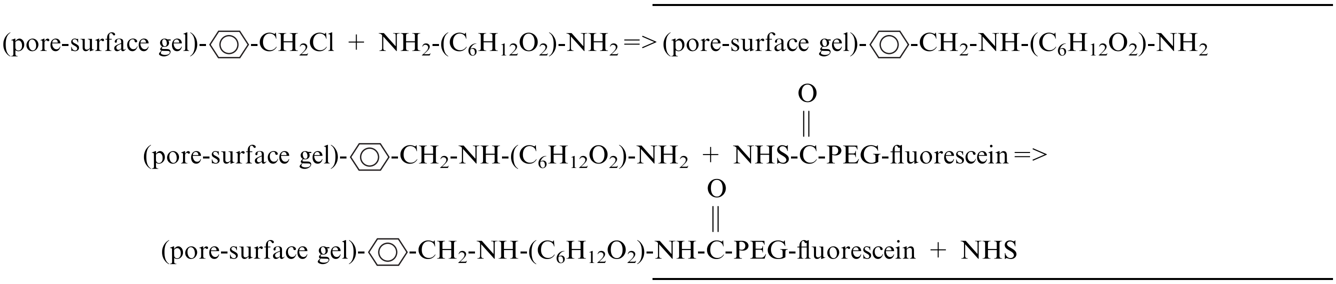

$$\text{(pore-surface gel)-}\langle\bigcirc\rangle\text{-CH}_2\text{Cl} + \text{NH}_2\text{-(C}_6\text{H}_{12}\text{O}_2\text{)-NH}_2 \Rightarrow \text{(pore-surface gel)-}\langle\bigcirc\rangle\text{-CH}_2\text{-NH-(C}_6\text{H}_{12}\text{O}_2\text{)-NH}_2$$

$$\text{(pore-surface gel)-}\langle\bigcirc\rangle\text{-CH}_2\text{-NH-(C}_6\text{H}_{12}\text{O}_2\text{)-NH}_2 + \text{NHS-}\overset{\overset{\text{O}}{\|}}{\text{C}}\text{-PEG-fluorescein} \Rightarrow$$

$$\text{(pore-surface gel)-}\langle\bigcirc\rangle\text{-CH}_2\text{-NH-(C}_6\text{H}_{12}\text{O}_2\text{)-NH-}\overset{\overset{\text{O}}{\|}}{\text{C}}\text{-PEG-fluorescein} + \text{NHS}$$

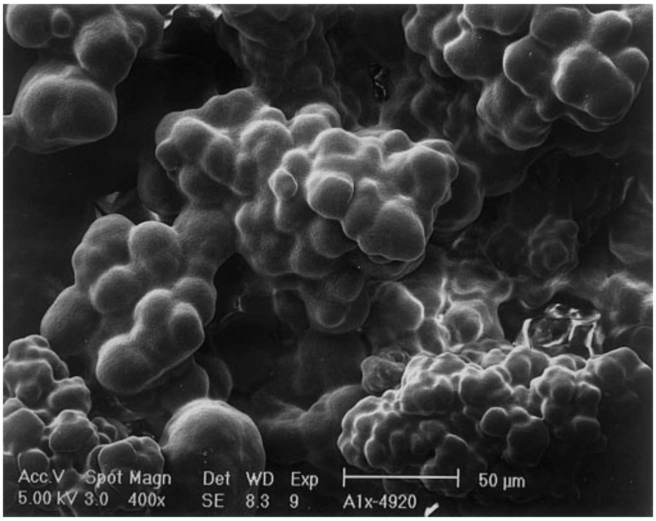

Fig. 1 A scanning electron photomicrograph (400×) of the macroporous ultrahigh molecular weight polyethylene (*UHMWPE*) (Porex X-4920)

Pore Surface Type	Probe Molecule	Probe-Surface Reaction	Comment
Ammonia FDRC Porex T^3 $R\text{-}NH_2$	5-(4,6-dichlorotriazinyl) aminofluorescein	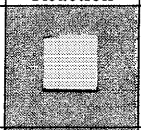	Staining shows covalent coupling of probe with putative $R\text{-}NH_2$ groups
Ammonia FDRC Porex T^3 $R\text{-}NH_2$	Fluorescein-5-isothiocyanate	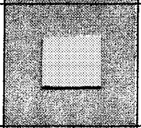	Staining shows covalent coupling of probe with putative $R\text{-}NH_2$ groups
Ammonia FDRC Porex T^3 blocked by N-acylation $R\text{-}NH\text{-}(C{=}O)\text{-}CH_3$	5-(4,6-dichlorotriazinyl) aminofluorescein	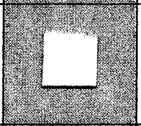	Little or no staining if surface amine groups are blocked by conversion to amides
Ammonia FDRC Porex T^3 blocked by N-acylation $R\text{-}NH\text{-}(C{=}O)\text{-}CH_3$	Fluorescein-5-isothiocyanate	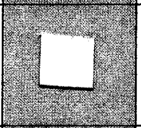	Little or no staining if surface amine groups are blocked by conversion to amides
Ammonia FDRC Porex T^3 $R\text{-}NH_2$	5-(4,6-dichlorotriazinyl) aminofluorescein + 1-ethylaminopropane	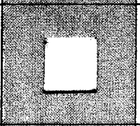	Little or no staining if amine reactive probe functionality is blocked
Ammonia FDRC Porex T^3 $R\text{-}NH_2$	Fluorescein-5-isothiocyanate + 1-ethylaminopropane	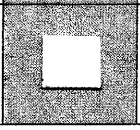	Little or no staining if amine reactive probe functionality is blocked

Fig. 2 Results of 5-(4,6-dichlorotriazinyl) aminofluorescein and fluorescein isothiocyanate staining reactions with ammonia flowing-discharge radical chemistry (*FDRC*) aminated macroporous UHMWPE material (Porex T^3)

reaction with a 5000 MW fluorescein-PEG-NHS ester after colloid coupling suggests that the properties of the surface-gel phase formed by covalent colloid coupling, solvent swelling, and derivitization are also uniform throughout the thickness of the stack. The control disks, untreated Porex X-4920, showed no significant colloid coupling or FITC reaction.

The data in Table 1 demonstrate successful construction of a pellicular monolith pore-surface gel phase in an FDRC aminated Porex X-4920 material as well as the uniformity throughout the porous matrix. As shown in Table 1, the colloid coupling proceeded to the extent of 14 mg/g of Porex. The specific pore surface area of the Porex is 1407 cm^2/g by gas adsorption, and 14 mg of spheres 0.46 μm in diameter occupy 58% of that area as a close-packed array. It follows that the yield of the polymer colloid coupling reaction is 58% of the geometric theoretical yield. The geometric theoretical yield can only be achieved on a perfectly flat surface on which the colloidal particles have sufficient mobility to pack into a crystalline array [20]. If the colloidal particles bind promptly on collision with the surface so that subsequent packing to form an ordered array is impossible, then a randomly distributed array of spheres will result and 56% is near the maximum possible surface coverage [20].

Solvent swelling and derivitization of the covalently coupled polymer colloid beads with the fluorescein-PEG-NHS ester molecule results in a pore-surface gel phase containing 74–76% fluorescein-PEG by weight, corresponding to 9 μmol fluorescein-PEG per gram of pellicular monolith. In contrast, ammonia FDRC aminated Porex X-4920 bound only 0.16 μmol fluorescein-PEG-NHS ester per gram of X-4920, demonstrating that the construction of the pore-surface gel phase produces a

Table 1 Uniformity of flowing-discharge radical chemistry (*FDRC*) pore-surface amination of Porex X-4920

Sample	FITC assay: umol/g reactive amine	Covalent colloid coupling mg(colloid) per gram Porex	Colloid + PEG-NHS ester: (5000 MW fluor-PEG-NHS) mg(colloid + PEG) per gram Porex
Amino FDRC top disk	0.060	15 mg/g	59 mg/g
Amino FDRC middle disk	0.061	14 mg/g	49 mg/g
Amino FDRC bottom disk	0.071	14 mg/g	59 mg/g
Control disk (Porex X-4920)	0.009	0.006 mg/g	NA

Table 2 Change in the hydraulic radius of Porex X-4920 resulting from construction of the pellicular monolith pore-surface gel phase

Material	Hydraulic radius for H_2O (μm)	Hydraulic radius for tetrahydrofuran (μm)
Porex X-4920 ammonia FDRC only	23.2 ± 1.5	25.8 ± 2.8
Porex X-4920 ammonia FDRC + pore-surface gel phase (Table 1, column 4)	18.8 ± 1	19.0 ± 1.4

56-fold increase in the useful functional group capacity for covalent capture of the 5000 MW fluorescein-PEG-NHS ester.

After colloid coupling, the pellicular monolith precursor should contain 55 μmol/g reactive benzyl chloride groups, based on the composition of the polymer colloid particles. The net yield of the pore-surface gel phase derivitization process is 16% based on the benzyl chloride content of the covalently coupled polymer colloid particles. On average, every sixth benzyl chloride repeat unit in the copolymer (i.e., every 12th repeat unit) chain is linked to a 5000 MW fluorescein-PEG molecule. On average, the macromolecular architecture of the pore-surface gel phase is most probably comb-like between the cross-link points. Simple reaction of the fluorescein-PEG-NHS molecules with the external surfaces of covalently coupled polymer colloid particles cannot account for the high fluorescein-PEG content of the final pore-surface gel phase or the relatively high yield of the derivitization reactions. Derivitization throughout a significant volume fraction of the pore-surface gel phase is the most likely explanation.

Measurements of fluid flow rates through short columns of ammonia FDRC Porex X-4920 and X-4920 containing the fluorescein-PEG derivitized pore-surface gel phase showed that the material containing the pore-surface gel phase offered a somewhat greater resistance to fluid flow. Some increase in resistance to fluid flow is expected in the pellicular monolith because construction of the pore-surface gel phase should reduce the average pore diameter.

The hydraulic radius concept is often used to calculate flow through channels and porous beds of differing geometry [21, 22] and can be used to relate the observed changes in fluid flow rate to changes in average pore diameter. The expression for hydraulic radius relates the average flow velocity of a fluid in a porous medium to the pressure force driving the flow, the viscosity of the fluid, the length of the porous bed, and the hydraulic radius of the bed (a measure of pore size).

The hydraulic radius is defined as $R_\mathrm{h} = V/A$, where V is the volume available for flow and A is the surface area in contact with fluid. The average fluid flow velocity, v, in a porous matrix is related to the hydraulic radius by the following expression [21, 22].

$$v = (\Delta P R_\mathrm{h}^2)T/2\eta lm \ ,$$

where, Δp is the pressure drop through the porous bed, η is the viscosity of the fluid, l is the length of the porous bed, T is the tortuosity factor (accounts for flow around particles in the porous bed), and m is the shape factor (corrects for noncircular flow channel).

The shape factor, m, and the tortuosity factor, T, depend on the detailed structure of the porous medium through which the fluid is flowing and a priori calculation of T and m is uncertain at best [22]. Values of T reported in the literature range from 0.3 to 0.6 and values of m range from 1.25 to 1.5 [22]. Given the uncertainty in T and m and the fact that the value of $(m/T)^{1/2}$ is close to 1 for reasonable choices of T and m, we have set $(m/T)^{1/2}$ equal to 1 for the purpose of calculating R_h.

The average fluid velocity, v, is defined in terms of the measured volumetric flow rate, Q, as follows:

$$v = Q/C\varepsilon \ ,$$

where C is the geometric cross-sectional area of the column and ε is the interparticle porosity or void fraction of the porous bed. The measured value of ε for Porex X-4920, 0.425, was used for calculating v in all cases.

The results of repeated hydraulic radius measurements on ammonia FDRC Porex X-4920 with and without the pore-surface gel phase are shown in Table 2, along with the corresponding experimental error terms. Construction of the pore-surface gel phase results in a small, but significant, decrease in the hydraulic radius so that the resulting pellicular monolith has fluid flow properties comparable to the starting material. The observed change in hydraulic radius suggests that the thickness of the solvent swollen pore-surface gel phase is 4 μm in water and 5 μm in THF. The covalently coupled polymer colloid particles have swollen approximately tenfold as a result of solvent swelling and PEG derivitization.

Summary and conclusions

The interstitial pore surfaces of thick macroporous UHMWPE materials have been uniformly functionalized throughout by ammonia FDRC. Ammonia FDRC was shown to uniformly aminate the pore surfaces of a 30-μm nominal pore size UHMWPE filter material (Porex X-4920) through a thickness of 0.48 cm such that XPS, reactive dye, and reactive polymer colloid measurements showed less than 17% variation through the thickness to the material.

A macroporous UHMWPE material functionalized by ammonia FDRC was used as the platform for construction of a pellicular monolith. Covalent coupling of amine reactive polymer colloid particles (0.46 μm mean diameter) to the aminated pore surfaces of the UHMWPE material was achieved with yields near the theoretical limit. Subsequent solvent swelling and derivitization of the covalently coupled polymer colloid particles showed that a 5000 MW fluorescein-PEG-NHS ester could enter the pore-surface gel phase and react to produce a PEG-modified pore-surface gel phase that was up to 76% PEG by weight. The low degree of cross-linking (0.2% by composition) of the polymer colloid assured the high degree of swelling which permits access of a relatively large macromolecular reagent such as the 5000 MW fluorescein-PEG-NHS ester.

Hydraulic radius measurements before and after the construction of the fluorescein-PEG modified pore-surface gel phase show that the lightly cross-linked polymer colloid particles had swollen to form a pore-surface gel phase of the order of 5-μm thick in both water and THF. The starting polymer colloid particles were 0.46 μm in diameter so that a net swelling factor of about 10 is indicated.

The type of pellicular monolith structure reported here should be widely applicable in several areas of chemistry, medical technology, and biotechnology. The solid-phase synthesis of oligonucleotides on pellicular monolith materials of the type reported here is presented elsewhere [23]. Chromatographic applications of the pellicular monolith to the separation of oligonucleotides, plasmids, and colloidal particles are also presented elsewhere. The ability to control thickness, functional group content, and swelling properties of covalently immobilized surface phases using the methods presented here should also prove generally useful in the development of high-performance surface phases for medical devices.

References

1. Huber CG, Stimpf E, Oefner PI, Bonn GK (1996) LC GC 14: 114–127
2. Koontz SL, Leger LJ, Wu C, Cross JB, Jurgensen CW (1994) In: Proceedings of the NASA Johnson Space Center Dual-Use Technology Conference. NASA Johnson Space Center Publications Office
3. Koontz SL (1994) US Patent 5,332,551
4. Koontz SL (1998) US Patent 5,798,261
5. Fitch RM (1997) Polymer colloids. Academic Press, San Diego
6. Svec F, Frechet JMJ (1996) Science 273: 205–211
7. Bergbreiter DE (1994) Prog Polym Sci 19: 529–560
8. Foerch R, McIntyre NS, Hunter DH (1990) J Polym Sci 28: 193–204
9. Foerch R, Izawa J, Spears G (1991) J Adhes Sci Technol 5: 549–564
10. Strobel M, Walzak MJ, Hill JM, Lin A, Karbashewski E, Lyons CS (1995) J Adhes Sci Technol 9: 365–383
11. Sapieha S, Cerny J, Klemberg-Sapieha JE, Martinu I (1993) J Adhes 42: 91–102
12. Yao Y, Liu X, Zhu Y (1993) J Appl Polym Sci 48: 57–65
13. Chu T-J, Caldwell KD, Weiss RB, Gesteland RF, Pitt WG (1992) Electrophoresis 13: 105–114
14. Denes F (1997) TRIP 5: 23–31
15. Inagaki N (1966) Plasma surface modification and plasma polymerization Technomic, Lancaster, pp 233–259
16. Deshmukh SC, Economou DJ (1993) J Vac Sci Technol B 11: 206–215
17. Kerr AS, Moss SS (ed) (1981) CRC handbook of bimolecular and termolecular gas reactions, vols 1 and 2, CRC Press, Boca Raton, Florida
18. Garbassi F, Morra M, Occheillo E (1998) Polymer surfaces. Wiley, Chichester, pp 71–155
19. Hermanson GT (1996) Bioconjugate techniques. Academic Press, San Diego, pp 137–145
20. Trezadel M, Slomkowski S, (1996) Colloid Polym Sci 274: 1109–1118
21. Karger BL, Snyder LR, Horvath C (1973) An introduction to separation science. Wiley, New York, pp 90–92
22. Bear J (1988) Dynamics of fluids in porous media. Dover, New York, pp 165–167
23. Devivar RV, Koontz SL, Peltier WJ, Pearson JE, Guillory TA, Fabricant JD (1999) Bioorg Med Chem Lett (in press)